Iğdır Üniversitesi Fen Bilimleri Enstitüsü Dergisi, 14(4), 1672-1683, 2024
Journal of the Institute of Science and Technology, 14(4), 1672-1683, 2024

ISSN: 2146-0574, eISSN: 2536-4618

Chemistry **DOI: 10.21597/jist.1514004**

Research Article

Received: 10.07.2024 **Accepted: 04.09.2024**

To Cite: Hüssein, Z. T. A. & Güler, M. (2024). Development of Non-Enzymatic Electrochemical p-Nitrophenol Sensor Based on Carboxylated Graphene Oxide Modified Glassy Carbon Electrode. *Journal of the Institute of Science and Technology*, 14(4), 1672-1683.

Development of Non-Enzymatic Electrochemical P-Nitrophenol Sensor Based on Carboxylated Graphene Oxide Modified Glassy Carbon Electrode

Zhivan Tayeb Ali HUSSEIN[1], Muhammet GÜLER[1*]

Highlights:

- A novel p-nitrophenol sensor was fabricated
- Glassy carbon electrode was modified using carboxylated graphene oxide
- The sensor was used for detection of p-nitrophenol in water samples

Keywords:

- Electrochemical sensor
- Carboxylated graphene oxide
- p-Nitrophenol

ABSTRACT:

The current work reports a new electrochemical p-nitrophenol (p-NP) sensor which depends upon the carboxyl functionalized graphene oxide (GO-COOH) modified of glassy carbon electrode (GCE). Scanning electron microscopy (SEM) and Fourier transform infrared spectroscopy (FTIR) were performed to examine the morphology of GO-COOH. The GO-COOH/GCE sensor was electrochemically characterized by means of chronoamperometry, electrochemical impedance spectroscopy (EIS), cyclic voltammetry (CV), and linear sweep voltammetry (LSV). A distinct cathodic peak of p-NP was seen on the GO-COOH/GCE in 0.1 M phosphate buffer solution (pH 6.5). The sensor displayed three dynamic linear ranges for p-NP under optimum conductions. The linear detection ranges were 2.0×10^{-7} - 2.95×10^{-6} M, 2.95×10^{-6} – 2.74×10^{-4} M, and 2.74×10^{-4} – 7.25×10^{-4} M with the sensitivities of 39622.1 A/Mm^2, 9959.3 A/Mm^2, and 6395 A/Mm^2, respectively. It was found that detection limit (LOD) was 5.3×10^{-8} M at a signal to noise ratio of 3. The GO-COOH/GCE demonstrated satisfactory performance factors such as selectivity and repeatability. Additionally, the GO-COOH/GCE sensor was demonstrated to be utilized to electrochemically determine p-NP in a variety of water samples.

[1]Zhivan Tayeb Ali HUSSEIN (**Orcid ID:** 0009-0002-0608-6047), Muhammet GÜLER (**Orcid ID**: 0000-0002-1040-8988). Van Yuzuncu Yil University, Faculty of Science, Department of Chemistry, Van,Turkey

***Corresponding Author:** Muhammet Güler, e-mail: mguler@yyu.edu.tr

This study was produced from Zhivan Tayeb Ali Hussein's Master's thesis.

INTRODUCTION

Phenols have been widely utilized in numerous industries for the manufacturing of chemicals, either as intermediates or basic materials. This implied that certain phenols got into the soil and water and contaminated them. Nitrophenols are organic compounds have poisonous and inhibitory properties, and frequently utilized in the production of commercially important products such as drugs and pesticides (Schummer et al., 2009). Owing to the great toxicity of p-nitrophenol (p-NP), it can severely damage the environment and living organisms. In addition, p-NP is not readily broken down by microbes and can endure in the natural world. Owing to the toxicity, the usage of p-NP by people can result in a number of diseases such as headaches, sickness, cyanosis, and drowsiness (Xu et al., 2011). Thus, getting rid of p-NP from soil and water is an important mater. As a result, environmental p-NP monitoring is crucial for both human health and water safety.

Currently, p-NP in environmental samples can be determined using a variety of methods, including capillary electrophoresis (Zhang et al., 2012), enzyme based on immunosorbent assay (Tingry et al., 2006), fluorescence (Yang et al., 2019), HPLC (Almási et al., 2006), and flow injection analysis (Leon-Gonzalez et al., 1992). Unfortunately, these methods are not appropriate for on-site analysis since they require costly devices and taking a lot of time sample processing. Thus, it is vital to construct a novel p-NP detection method that is more affordable and time-efficient.

Due to its benefits—small instruments, easy operation, high sensitivity, and quick response—electrochemical sensing has drawn a lot of interest in p-NP detection. To date, electrochemical sensors have been utilized in many fields. For examples, they have been used for determination of biologically active compounds such as glucose, dopamine, ascorbic acid, riboflavin and electrochemically active drugs such as paracetamol and metronidazole. However, there are significant interference problems and a large overpotential needed for p-NP measurement on bare working electrodes (Yang et al., 2011). As a result, electrodes with modifications were suggested for p-NP measurement. In the sensor and biosensor technologies, various working electrodes have been performed to detect p-NP, including conducting polymers (Saadati et al., 2018), carbon-depending composites (graphene, nanotubes) (Li et al., 2012), noble metal nanoparticles (Hira et al., 2019), and metal oxides nanoparticles (Anbumannan et al., 2019). To detect p-NP, it is still preferable to create novel nanomaterials with straightforward production techniques and superior electrocatalytic performance.

Carbon depending materials such as graphene is among the most preferred materials for detection of electrochemically active compounds because of its remarkable properties and inexpensive of graphite powder. These characteristics include low fouling, high specific surface area, quick electron transfer rate, and excellent electroconductivity at a reasonable price. GO is widely utilized for the modification electrode materials Chen at al., 2010). For this, graphite powder is used as the starting material to synthesize GO by means of the modified Hummer's method. GO includes functional groups such as carboxyl and hydroxy, which allows it to disperse in solvent and presents many electroactive sites for target analyte(s) (Tavakoli et al., 2023). Since GO has limited electrical conductivity, using only GO to modify the working electrode surface gives a low electroactive surface area and sensitivity. Therefore, in many works performed to date, either graphene oxide was reduced (Shamkhalichenar and Choi, 2020) or metal/metal oxide nanoparticles were deposited on the graphene (Fadillah et al., 2020; Jahromi et al., 2020).

In one article performed by Li and his co-workers, a p-NP sensor was obtained by using GO to modify glassy carbon working electrode. The electrocatalytic characteristics of the electrode were searched by means of EIS, CV, and LSV. The GO/GCE exhibited a linear determination range for p-NP

between 1.0×10^{-7} and 1.2×10^{-4} M with detection limit of 2.0×10^{-8} M (Li et al., 2012). In another study, MWCNTs were utilized for modification of working electrode. The linear range was estimated to be between 2.0×10^{-6} M and 4.0×10^{-3} M with the detection limit of 4.0×10^{-7} M. Also, artificial samples were used for the practicability of the sensor (Luo et al., 2008).

In the present study, p-NP was detected by means of a GCE modified with GO-COOH. The GO-COOH material increased the electroactive area of the bare working electrode. In addition, GO-COOH/GCE electrochemical sensor showed a wide linear determination range for p-NP when compared to previously performed sensors (Table 1).

MATERIALS AND METHODS

Graphite powder (Gr), potassium chloride (KCI), $K_4[Fe(CN)_6].3H_2O$, N, N-dimethyl formamide (DMF), K_2CO_3, $CaCl_2$, bisphenol A (BPA), fructose (Fruc), hydroquinone (HQ), phenol, ascorbic acid (AA), pyrocatechol (PC), $K_3[Fe(CN)_6]$, glucose (Glu), and histidine (His) were acquired from Sigma Comp. 4-nitrophenol (p-nitrophenol; p-NP) was bought from Thermo Scientific Chemicals. All additional compounds used in the study, including nitric acid (HNO_3) and chloroacetic acid ($ClCH_2COOH$), were purchased from Merck®.

For electrochemical experiments, an Autolab PGSTAT128N with the FRA 32M was used. The platinum (Pt) wire counter electrode, GCE, and Ag/AgCl (3 M KCl) reference electrode were obtained from BASi Corporation. The morphology of GO and GO-COOH were evaluated by means of SEM (Zeiss sigma 300) and FTIR. To attain uniform dispersion, an ultrasonic bath (VWR USC300TH) was employed.

Synthesis of Graphene Oxide

Graphene oxide (GO) was obtained by means of the improved Hummer's method (Marcano et al., 2010). 270 mL of H_2SO_4/H_3PO_4 mixture in the ratio of (9:1) and 3 g of graphite powder (Gr) were supplemented to a beaker for this purpose. Next, the mixture was slowly supplemented with 18 g of $KMnO_4$. In an oil bath, the mixture was warmed up to 50 ºC and stirred continuously for 24 h. Following cooling of the mixture to the laboratory temperature, 400 mL of distilled water were gradually supplemented to it. Subsequently, the reaction was terminated by adding 5 mL of 35% hydrogen peroxide to the reaction medium. The mixture was centrifugated for 20 minutes at 8000 rpm. 500 mL of 10% hydrogen chloride was put into the solid substance, and it was stirred for some time. The mixture was centrifuged several times for 20 minutes at 8000 rpm until its pH vale was about neutral. The solid was then dried at 60 ºC in the oven.

Synthesis of Carboxylated Graphene Oxide

1.5 g of GO was supplemented to 50 mL of ultrapure water andstirred and sonicated for 2 hours, respectively. Afterwards, to the mixture, 3 g of $ClCH_2COOH$ and 8 g of KOH were supplemented and stirred for some time. After filtering, the mixture was cleaned with ethanol and water, respectively. Finally, carboxylated graphene oxide (GO-COOH), the black solid, was dried at 60 ºC in the oven (Xu et al., 2016; Saleem and Guler, 2019).

Modification of Bare Electrode

Before modification, the GCE was polished with Al_2O_3, washed and cleaned using an ultrasonic bath in HNO_3/H_2O (1:1), and then in ethanol for five minutes. This process was repeated until the surface of GCE was mirror-like. To 1 ml of DMF, 1.0 mg of GO-COOH was supplemented and sonicated till a uniform dispersion was achieved. Following that, 4 µL of the mixture was drop-casted on the bare

electrode, and it was dried at 50 °C in the vacuum oven. The GO modified GCE was prepared using the same procedure as mentioned above.

RESULTS AND DISCUSSION

FTIR and SEM were utilized to characterize GO and GO-COOH. GO exhibits three intense peaks at around 1037, 1620, and 1721 1/cm, as can be displayed in Figure 1a. The stretching vibration of the C=O group is appeared at 1721 1/cm. The vibration modes of C=C and C-O groups is seen at 1620 1/cm and 1037 1/cm, respectively. The stretching modes of the OH and C-OH groups are appeared at 1161 and 3340 1/cm, respectively (Marcano et al., 2010). Figure 1b exhibits the FTIR spectra of GO-COOH. In comparison to the GO spectra, the distinctive vibration peak of C-O at 1055 1/cm diminished and shifted to a more positive value. The in-plane bending mode of the OH group is shown at 1354 1/cm. A prominent peak at 1577 1/cm is seen in the synthesized GO-COOH, indicating that additional carboxylic groups were forming on the GO (Xu et al., 2016; Saleem and Guler, 2019).

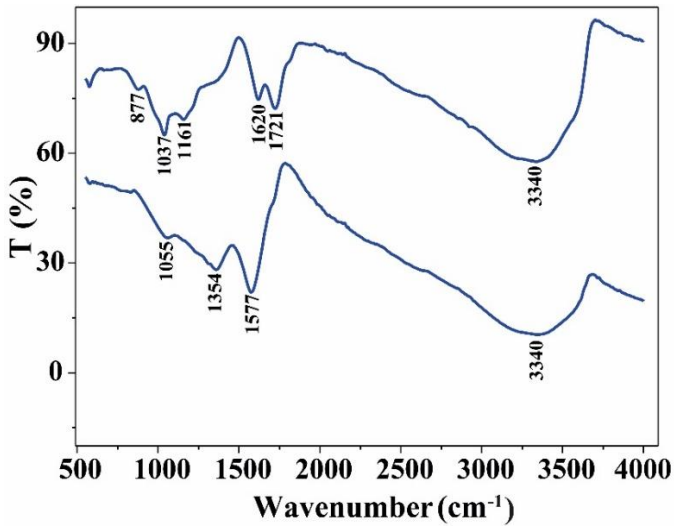

Figure 1. FTIR graph of (a) graphene oxide and (b) carboxyl functionalized graphene oxide

The SEM pictures of Gr, GO, and GO-COOH are displayed in Figure 2. A typical SEM pictures of Gr is shown in Figure 2a. The Gr has a smooth and flat surface. By van der Waals interactions, each layer is closely linked. GO has a multilayer microstructure with creases and surface defects, as seen in Figure 2b. This could be as a result of epoxy, hydroxyl, and carboxyl groups. Because of the availability of these groups, the interlayer distance of the Gr increases and its ground-in layer microstructure was destroyed, which results in the wrinkle structure of GO (Gong et al., 2015). As shown in Figures 2c and 2d, the surface morphology of GO changed after carboxylation. The presence of several irregular creases and a rough surface on GO-COOH may be ascribed to the various carboxyl groups that were introduced throughout the chemical reaction process. Furthermore, it can be claimed that GO was exfoliated during the carboxylation process.

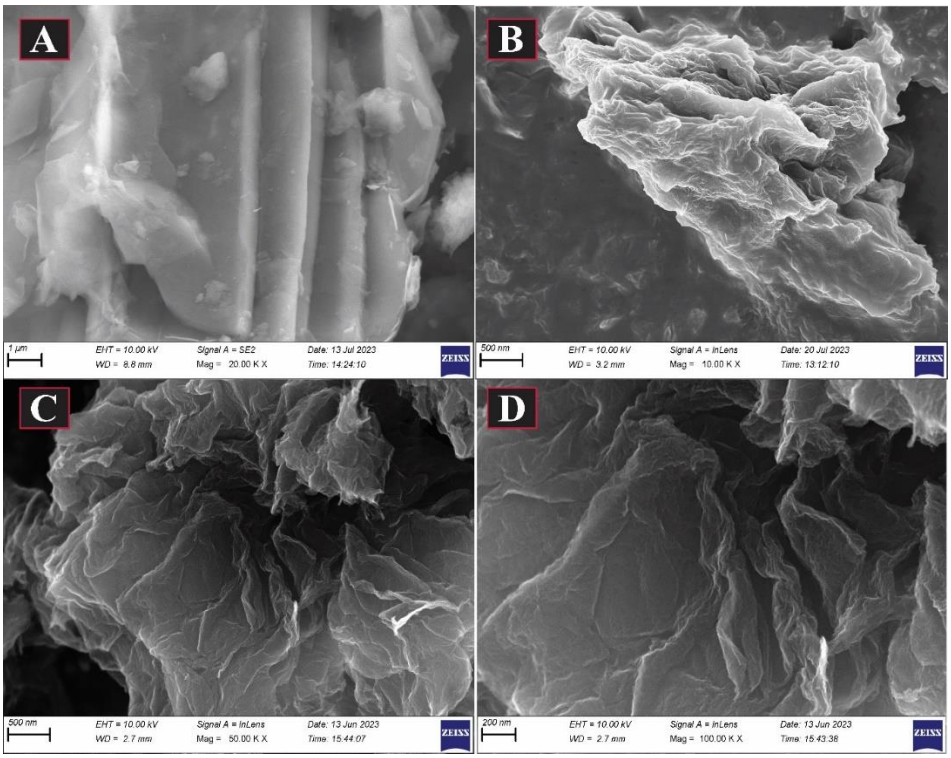

Figure 2. SEM images of (A) Gr, (B) GO, and (C, D) GO-COOH

In the study, the electrocatalytic activity of the working electrodes were investigated by means of both EIS and CV techniques. The Nyquist plot produced by the EIS provides significant information for sensor. The graph contains a real part (Z′) on the x-axis and an imaginary part (-Z″) on the y-axis. Typically, at low frequencies, the graph is linear, whereas at high frequencies, it is semicircular. The process limited to electron transfer is accounted for by the semicircle component. The diameter value of semicircle corresponds to charge transfer resistance (Rct) of the sensor (Gandouzi et al., 2018). The diffusion process is supported by the linear portion. The Nyquist graph of the $[Fe(CN)_6]^{3-}/[Fe(CN)_6]^{4-}$ redox probe obtained on the working electrodes is displayed in Figure 3A. The estimated Rct values on GCE (Figure 3Aa), GO/GCE (Figure 3Ab), and GO-COOH/GCE (Figure 3Ac), were 150 Ω, 338 Ω, and 83.6 Ω, respectively. The fact that the GO-COOH/GCE working electrode showed the lowest Rct value indicates that GO-COOH accelerated the rate of electron transport.

For years now, cyclic voltammetry has been the mainstay of electrochemists in labs all around the world. It is utilized to evaluate the thermodynamic and kinetic properties of any type of material which is electrochemically active or has active group(s) on it that can be oxidized/reduced or both. It is used to determine operating parameters for electrochemical investigations, to find electrocatalysts for a variety of applications. Also, it is performed to estimate the reaction mechanisms. Due to a wide using areas, CV has attracted the attention and interest of many scientists. In this study, CV was used to determine possible reduction and oxidation reactions of the target analyte (Compton and Banks, 2018). The cyclic voltammograms of the redox pair, achieved on the working electrodes, are shown in Figure 3B. As shown in Figures 3Ba, 3Bb, and 3Bc, the oxidation peak current values of the redox probe were 4.81×10^{-5} A on GCE, 4.17×10^{-5} A on GO/GCE, and 5.71×10^{-5} A on GO-COOH/GCE. As displayed in Figure 3A and Figure 3B, it is concluded that the Rct decreases as the anodic peak current of the probe increases, which demonstrates that the relationship between Rct and the electron transfer rate is inverse.

In order to search the electrocatalytic responses of bare and modified working electrodes to the analyte, CVs were obtained in the buffer solution (Figure 3C). As shown in Figures 3Ca, 3Cb, and 3Cc,

the cathodic peak value value of p-NP to 4-hydroxylaminophenol was 4.39×10^{-6} A on GCE, 1.15×10^{-5} A on GO/GCE, and 4.43×10^{-5} A on GO-COOH/GCE. The voltammograms indicated that the GO-COOH/GCE sensor exhibited the maximum peak current response to the analyte.

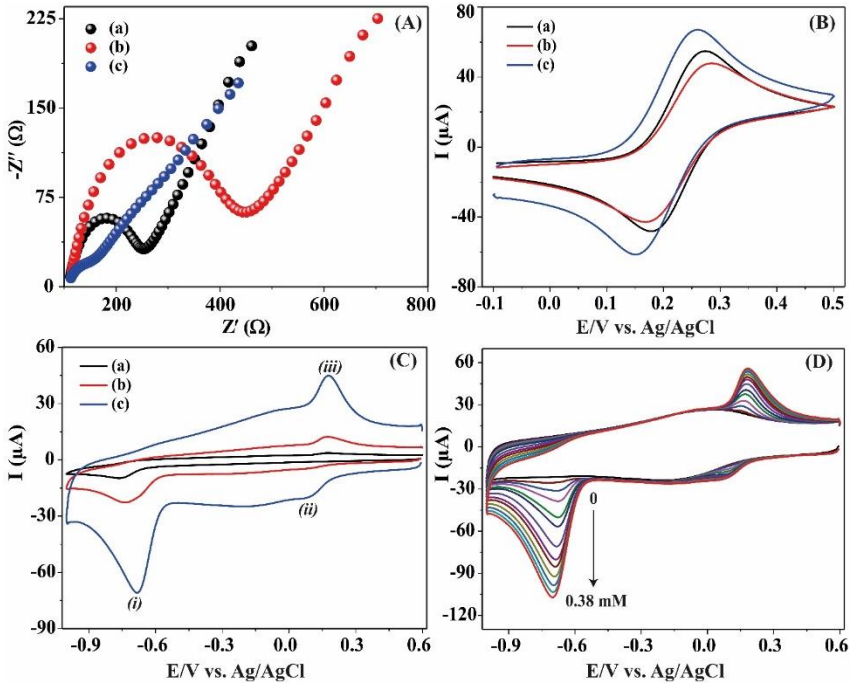

Figure 3. (A) Nyquist graph of (a) GCE, (b) GO/GCE, and (c) GO-COOH/GCE and (B) CVs of (a) GCE, (b) GO/GCE, and (c) GO-COOH/GCE obtained in 5.0×10^{-3} M redox probe containing 0.1 M KCl. (C) CVs obtained on (a) GCE, (b) GO/GCE, and (c) GO-COOH/GCE in 0.1 M phosphate buffer (PBS, pH 6.5) including 2.0×10^{-4} M p-NP at the sweep rate of 0.05 V/s. (D) CV responses of GO-COOH/GCE to different concentrations of p-NP

So as to assess the reaction mechanism of p-NP on the electrode prepared by GO-COOH, cyclic voltammograms were recorded in 0.1 M PBS (pH 6.5) containing p-NP. In the scanning step from 0.6 to -1.0 V at the sweep rate of 0.05 V/s, two reduction peaks were observed at -0.684 V (i) and 0.0921 V (ii), and one oxidation peak at 0.1776 V (iii), as shown in Figure 3C. The peak (iii) at 0.1776 V and the peak (ii) at 0.0921 V form a redox couple during the reverse scan. Taking these findings into account, the following reactions provide a possible reaction mechanism (Dighole et al., 2020).

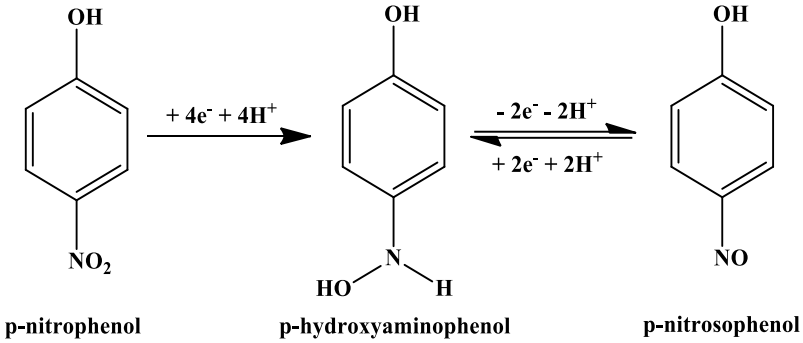

Figure 3D displays the cyclic voltammograms that were achieved on GO-COOH/GCE in the buffer solution including p-NP (ranging from 0 to 3.8×10^{-4} M).

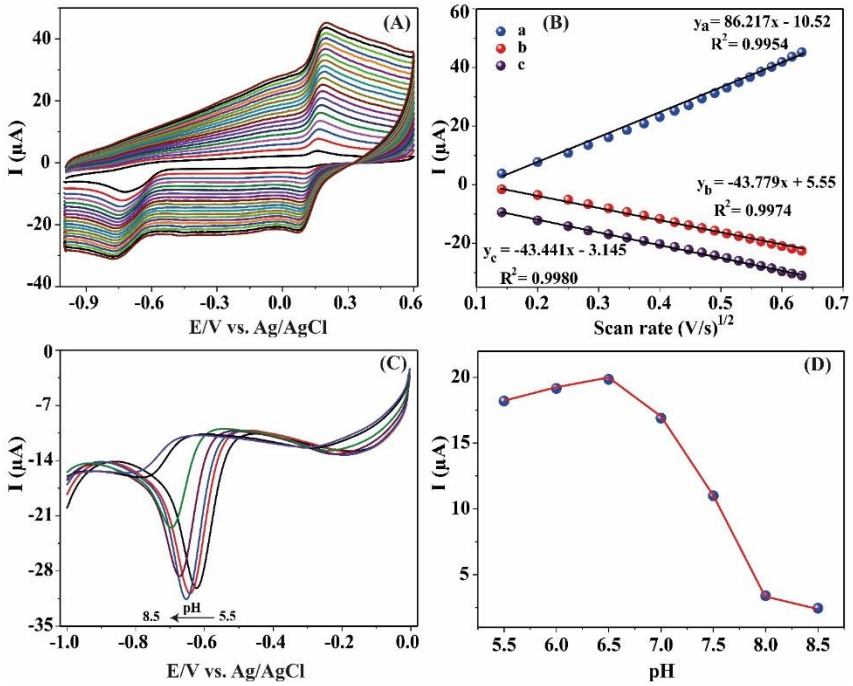

Figure 4. (A) CV responses of GO-COOH/GCE obtained at various sweep rates (0.02 – 0.4 V/s). (B) Current *versus* sweep rate $(V/s)^{1/2}$ graph. (C) Linear sweep voltammograms of p-NP achieved in 0.1 phosphate buffer solution with various pH values (5.5-8.5). (D) Current *versus* pH graph

Cyclic voltammograms were recorded by using various sweep rates (0.02 - 0.4 V/s) in 0.1 M phosphate buffer solution (pH 6.5) including p-NP so as to examine the kinetics of the p-NP electrode reaction on the GO-COOH/GCE sensor. The anodic peak current value of 4-hydroxyaminophenol and the cathodic peak values of p-NP and 4-nitrosophenol both enhanced when the sweep rate enhanced, as depicted in Figure 4A. The square root of the sweep rate and the values of the oxidation/reduction peak currents are linearly related, as seen in Figure 4B, which suggests that the diffusion-controlled electrode reaction takes place on GO-COOH/GCE (Dighole et al., 2020).

It is important to know the pH value of the used buffer solution in which the reactions occur. In particular, the sensitivity of the sensor is influenced by the pH of the solution. Consequently, 0.1 M PBS (phosphate buffer solution) with varying pH values (5.5-8.5) was prepared in our study. Linear sweep voltammetry was performed to assess the influence of pH value on the electrochemical reduction of p-NP at the GO-COOH/GCE working electrode (Figure 4C). As demonstrated in Figure 4D, the cathodic peak current of p-NP enhanced with the increase of pH from 5.5 to 6.5. The maximum cathodic peak value was recorded at pH 6.5. With a further enhance in the pH (from 7.0 to 8.5), the current value decreased. Thus, pH 6.5 was selected for further studies.

By using the amperometric method (Figure 5A), the fabricated GO-COOH/GCE sensor was performed to determine p-NP. The electrochemical responses were recorded following a step-by-step addition of p-NP to the N_2-saturated 0.1 M phosphate buffer solution (pH 6.5). The working electrode rotated at 1500 rpm. According to Figure 5B, the sensor displayed three linear determination ranges for p-NP. The first linear graph was between 2.0×10^{-7} M and 2.95×10^{-6} M and the sensitivity was computed to be 39622.1 A/Mm^2. The graph's linear equation was found as follows (Figure 5C).

$$I(\mu A) = 6.815 \times 10^{-5} C(M) + 0.0681 \ (R^2 = 0.9979) \quad (1)$$

The second linear detection range was between 2.95×10^{-6} M and 2.74×10^{-4} M. The sensitivity was 9959.3 A/Mm^2. The linear equation of the graph was as follows (Figure 5D):

$$I(\mu A) = 1.713 \times 10^{-5} C(M) + 2.7441 \ (R^2 = 0.9970) \quad (2)$$

The third linear detection range was between 2.74×10^{-4} M and 7.25×10^{-4} M. The sensitivity was estimated to be 6395 A/Mm^2. All sensitivities were calculated depending on the active surface area of the working electrode. The linear equation of the graph was as follows (Figure 5E):

$$I(\mu A) = 1.1 \times 10^{-5} C(M) + 19.803 \ (R^2 = 0.9970) \quad (3)$$

With the (S/N) ratio of 3, the detection limit (LOD) was computed to be 5.3×10^{-8} M. These findings show that, in comparison to earlier electrochemical studies, the GO-COOH/GCE sensor exhibited satisfactory electrochemical response to p-NP (Table 1).

The selectivity of a sensor is one of the extremely important parameters for the accurate determination of the target analyte because the analyte to be examined can be detected in real samples along with highly electroactive compounds such as glucose, folic acid, and ascorbic acid. Because of this, it is important to assess the selectivity of the sensor before examining the target analyte in the real samples. We have investigated the interfering effects of 4.0×10^{-5} µM phenol, hydroquinone (HQ), and bisphenol A (BPA), as well as 1.0×10^{-4} µM glycine (Gly), Na^+, K^+, Cl^-, Glu, Ca^{2+}, CO_3^{2-}, pyrocatechol (PC), and ascorbic acid (AA) on the GO-COOH/GCE response. As depicted in Figure 6, the sensor responses to these chemicals and ions were not very noteworthy. Thus, it can be concluded that in this kind of solution media, the sensor shows remarkable selectivity.

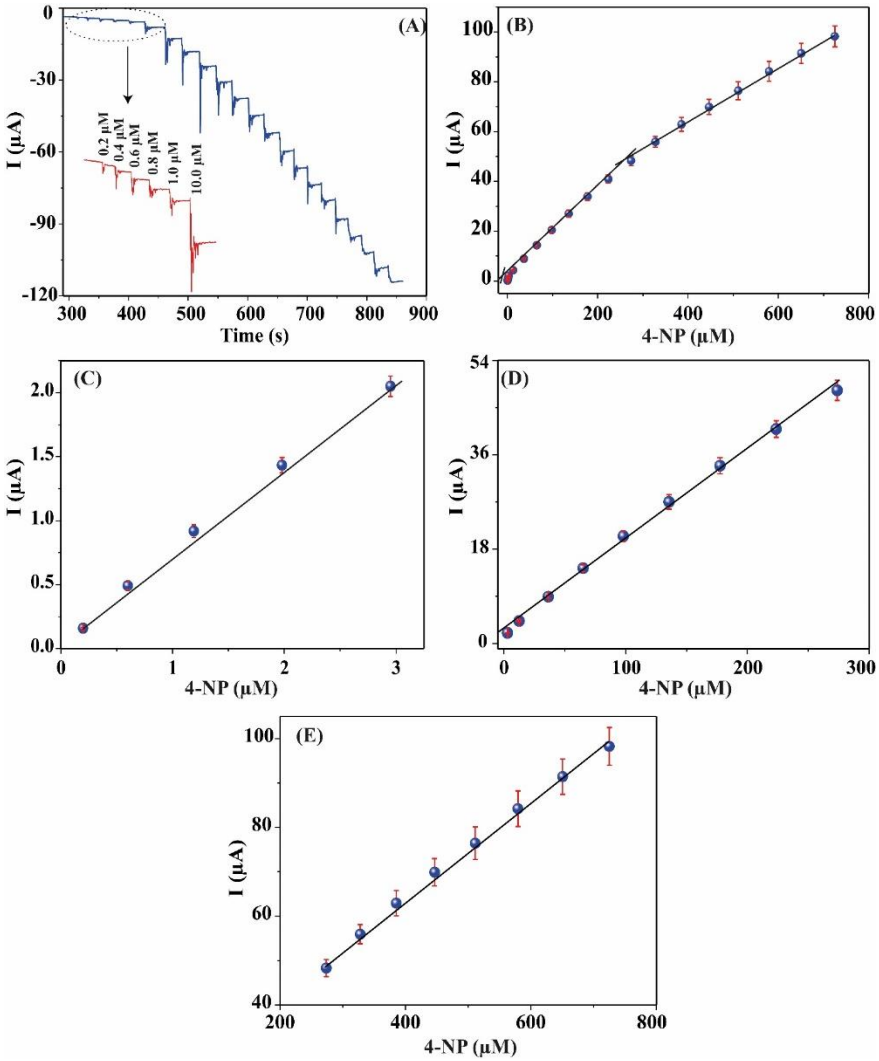

Figure 5. (A) Amperometric response of GO-COOH/GCE to p-NP. (B) Current versus concentration of p-NP graphs (2.0×10^{-7} M – 7.25×10^{-4} M), (C) from 2.0×10^{-7} to 2.95×10^{-6} M, (D) from 2.95×10^{-6} M to 2.74×10^{-4} M, and (E) from 2.74×10^{-4} M to 7.25×10^{-4} M

Table 1. The comparing of electrochemical responses of several electrochemical sensors previously reported

Working electrode	Linear detection range (M)	LOD (M)	Ref.
CD-SBA/CPA	2.0×10^{-7}-1.6×10^{-6}	1.0×10^{-8}	(Xu et al., 2011)
MWCNT-PDPA/GCE	8.9×10^{-6}-1.5×10^{-3}	-	(Yang et al., 2011)
MIP-PANI/GO	6.0×10^{-5}-1.4×10^{-4}	2.0×10^{-5}	(Saadati et al., 2018)
GO/GCE	1.0×10^{-7}-1.2×10^{-4}	2.0×10^{-8}	(Li et al., 2012)
AgPd@UiO-66-NH_2/GCE	1.0×10^{-4}-3.7×10^{-4}	3.2×10^{-5}	(Hira et al., 2019)
MWCNTs/MnO_2	3.0×10^{-5}-4.75×10^{-4}	6.44×10^{-7}	(Anbumannan et al., 2019)
Bi_2O_3@MWCNTs	1.0×10^{-3}-1.0×10^{-2}	1.0×10^{-7}	(Dighole et al., 2020)
SWNT/GCE	1.0×10^{-8}-5.0×10^{-6}	2.5×10^{-9}	(Yang, 2004)
Ni-NCs-PEI/GCE	6.0×10^{-8}-1.0×10^{-5} 1.0×10^{-5}-1.0×10^{-4}	4.0×10^{-9}	(He et al., 2022)
GO-COOH/GCE	2.0×10^{-7}-2.95×10^{-6} 2.95×10^{-6}-2.74×10^{-4} 2.74×10^{-4}-7.25×10^{-4}	5.3×10^{-8}	**This study**

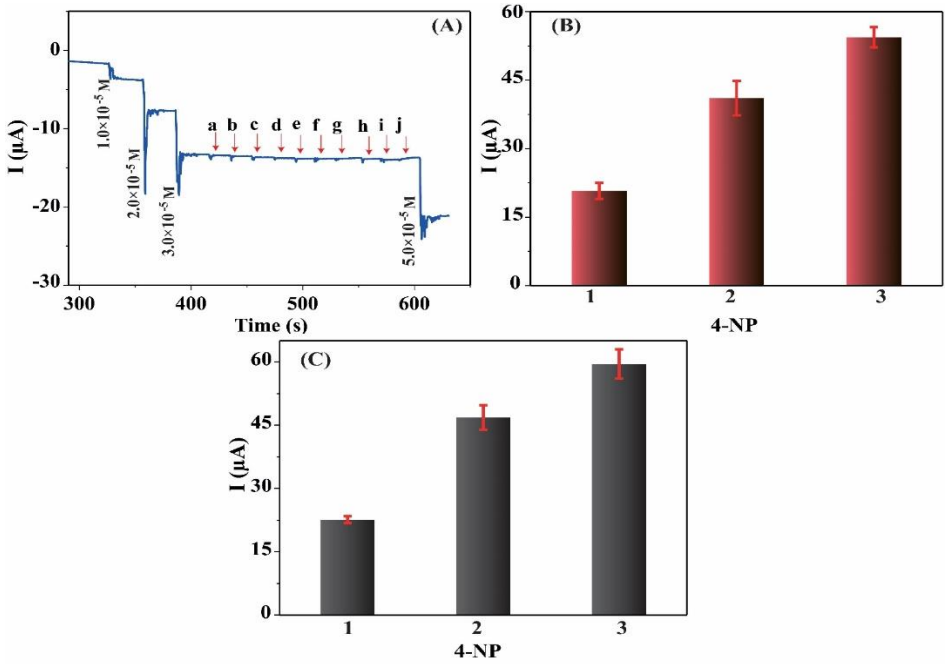

Figure 6. (A) Amperometric response of GO-COOH/GCE to p-NP (1.0×10^{-5}, 2.0×10^{-5}, 3.0×10^{-5}, and 5.0×10^{-5} M), 1.0×10^{-4} M Gly (a), Na^+ and Cl^- (b), Glu (c), K^+ and CO_3^{2-} (d), Ca^{2+} (e), PC (f), AA (g), and 4.0×10^{-5} M phenol (h), HQ (i), and BPA (j) in 0.1 M PBS with pH 6.5 at -0.66 V, (B) Repeatability of GO-COOH/GCE using different concentrations of p-NP, (C) Reproducibility of GO-COOH/GCE using different concentrations of p-NP

To investigate the repeatability of GO-COOH/GCE working electrode, five measurements were recorded by using the same electrode in the N_2-saturated 0.1 M phosphate buffer solution (pH 6.5) including different concentrations of p-NP (Figure 6B). The computed RSD values for the p-NP reduction current value were between 1.83 and 6.89%, suggesting that the sensor exhibits a satisfactory repeatability. Additionally, the reproducibility of the sensor was examined. For this, five distinct electrodes that were prepared under the same conditions were used to obtain the electrochemical reduction peak current of the analyte (Figure 6C). The RSD values of the current value were calculated to be between 2.92 and 4.95%, demonstrating that the sensor has good reproducibility. After 32 days, the fabricate sensor response to the analyte was determined to be 97.18%, indicating that the sensor exhibited good storage stability.

So as to examine the practical applicability of GO-COOH/GCE electrochemical sensor, groundwater and drinking water were used as real samples. Prior to tests, the water samples were filtrated to remove any contaminants. Subsequently, the water samples were mixed with a known quantity of p-

NP to prepare the spiked samples. Following that, amperometric measurements were obtained. To find the concentrations of p-NP in the prepared samples, the conventional standard addition method was applied. Table 2 displays the computed values. The recoveries in the drinking water were found to be between 98.57 and 104%. The recovery was calculated to be 104% for 3 μM p-NP, which is probably due to the deviation of the sensor in the low concentration of the analyte. In the groundwater, the recoveries were between 93.0 and 95.0%, respectively. These findings show that the GO-COOH/GCE can be performed to estimate p-NP in water samples.

Table 2. Detection of p-NP in different water samples (n = 5)

p-NP in groundwater	Added (μM)	Found (μM)	RSD (%)	Recovery (%)
i	0	Not detected	-	-
ii	3	2.84 ± 0.12	3.25	94.67
iii	7	6.65 ± 0.23	2.79	95
iv	13	12.15 ± 0.54	3.53	93.46
v	20	18.6 ± 0.91	3.94	93
p-NP in drinking water	**Added (μM)**	**Found (μM)**	**RSD (%)**	**Recovery (%)**
i	0	Not detected	-	-
ii	3	3.12 ± 0.29	7.46	104
iii	7	6.90 ± 0.40	4.67	98.57
iv	13	12.98 ± 0.25	1.55	99.85
v	20	19.81 ± 0.60	2.44	99.05

CONCLUSION

This study presents an electrochemical p-NP sensor depending on carboxylated graphene oxide modified of GCE. FTIR and SEM were used to characterize GO and GO-COOH. Amperometry, EIS, CV, and LSV were utilized in the electrochemical experiments. Three linear determination ranges for p-NP were displayed by the sensor: 2.0×10^{-7} to 2.95×10^{-6} M, 2.95×10^{-6} to 2.74×10^{-4} M, and 2.74×10^{-4} to 7.25×10^{-4} M. The LOD was computed to be 5.3×10^{-8} M. The sensor exhibited high sensitivity. The sensor showed strong repeatability with the RSD values between 1.83 and 6.89%, good reproducibility with the RSD values between 2.92 and 4.95%, and satisfactory selectivity. Additionally, the GO-COOH/GCE was utilized to estimate p-NP in drinking water and groundwater samples. The recoveries were estimated to be between 93% and 104%. Thus, the GO-COOH/GCE electrochemical sensor could be performed to detect p-NP in real water samples. In general, a novel p-NP electrochemical sensor was developed in the present work. It was observed that the carboxylated graphene oxide used for the modification of the working electrode enhanced the electroactive area of the bare electrode. Also, the carboxylated graphene oxide increased the sensitivity of the sensor to the target analyte. These results suggest that it might make an appropriate surface for the preparation of metal/metal oxide nanoparticles for further electrochemical sensor studies.

Conflict of Interest

There is no conflict of interest between the authors.

Author's Contributions

Muhammet Guler: Writing – original draft, Methodology, Supervision, Software, Data curation. Zhivan Tayeb Ali Hussein: Investigation, Data curation.

REFERENCES

Almási, A., Fischer, E., & Perjesi, P. (2006). A simple and rapid ion-pair HPLC method for simultaneous quantitation of 4-nitrophenol and its glucuronide and sulfate conjugates. *Journal of biochemical and biophysical methods*, 69 (1-2), 43-50.

Anbumannan, V., Dinesh, M., Kumar, R. R., & Suresh, K. (2019). Hierarchical α-MnO2 wrapped MWCNTs sensor for low level detection of p-nitrophenol in water. *Ceramics International*, 45 (17), 23097-23103.

Chen, D., Tang, L., Li, J. (2010). Graphene-based materials in electrochemistry. *Chemical Society Reviews*, 39 (8), 3157-3180.

Compton, R. G., & Banks, C. E. (2018). *Understanding voltammetry*. World Scientific.

Dighole, R. P., Munde, A. V., Mulik, B. B., & Sathe, B. R. (2020). Bi_2O_3 nanoparticles decorated carbon nanotube: an effective nanoelectrode for enhanced electrocatalytic 4-nitrophenol reduction. *Frontiers in Chemistry*, *8*, 325.

Fadillah, G., Wicaksono, W. P., Fatimah, I., & Saleh, T. A. (2020). A sensitive electrochemical sensor based on functionalized graphene oxide/SnO_2 for the determination of eugenol. *Microchemical Journal*, 159, 105353.

Gandouzi, I., Tertis, M., Cernat, A., Bakhrouf, A., Coros, M., Pruneanu, S., Cristea, C. (2018). Sensitive detection of pyoverdine with an electrochemical sensor based on electrochemically generated graphene functionalized with gold nanoparticles. *Bioelectrochemistry*, 120, 94-103.

Gong, Y., Li, D., Fu, Q., & Pan, C. (2015). Influence of graphene microstructures on electrochemical performance for supercapacitors. *Progress in Natural Science: Materials International*, 25 (5), 379-385.

Zhang, H., Wang, M., Zhao, J., & Shi, Z. (2012). Sandwich-type spontaneous injection of nitrophenols for capillary electrophoresis analysis. *Analytical Methods*, 4 (7), 2177-2182.

He, Q., Wang, B., Liu, J., Li, G., Long, Y., Zhang, G., & Liu, H. (2022). Nickel/nitrogen-doped carbon nanocomposites: Synthesis and electrochemical sensor for determination of p-nitrophenol in local environment. *Environmental Research*, 214, 114007.

Hira, S. A., Nallal, M., & Park, K. H. (2019). Fabrication of PdAg nanoparticle infused metal-organic framework for electrochemical and solution-chemical reduction and detection of toxic 4-nitrophenol. *Sensors and Actuators B: Chemical*, 298, 126861.

Jahromi, M. N., Tayadon, F., & Bagheri, H. (2020). A new electrochemical sensor based on an Au-Pd/reduced graphene oxide nanocomposite for determination of Parathion. *International Journal of Environmental Analytical Chemistry*, 100 (10), 1101-1117.

Li, J., Kuang, D., Feng, Y., Zhang, F., Xu, Z., & Liu, M. (2012). A graphene oxide-based electrochemical sensor for sensitive determination of 4-nitrophenol. *Journal of hazardous materials*, 201, 250-259.

Leon-Gonzalez, M. E., Pérez-Arribas, L. V., Santos-Delgado, M. J., & Polo-Díez, L. M. (1992). Simultaneous flow-injection determination of o-and p-nitrophenol using a photodiode-array detector. *Analytica chimica acta*, 258 (2), 269-273.

Luo, L. Q., Zou, X. L., Ding, Y. P., & Wu, Q. S. (2008). Derivative voltammetric direct simultaneous determination of nitrophenol isomers at a carbon nanotube modified electrode. *Sensors and Actuators B: Chemical*, 135 (1), 61-65.

Marcano, D. C., Kosynkin, D. V., Berlin, J. M., Sinitskii, A., Sun, Z., Slesarev, A., Alemany, L. B., Lu, W., & Tour, J. M. (2010). Improved synthesis of graphene oxide. *ACS nano*, 4 (8), 4806-4814.

Saadati, F., Ghahramani, F., Shayani-jam, H., Piri, F., & Yaftian, M. R. (2018). Synthesis and characterization of nanostructure molecularly imprinted polyaniline/graphene oxide composite as highly selective electrochemical sensor for detection of p-nitrophenol. *Journal of the Taiwan Institute of Chemical Engineers*, 86, 213-221.

Saleem, S. J., & Guler, M. (2019). Electroanalytical determination of paracetamol using Pd nanoparticles deposited on carboxylated graphene oxide modified glassy carbon electrode. *Electroanalysis*, 31 (11), 2187-2198.

Schummer, C., Groff, C., Al Chami, J., Jaber, F., & Millet, M. (2009). Analysis of phenols and nitrophenols in rainwater collected simultaneously on an urban and rural site in east of France. *Science of the total environment*, 407 (21), 5637-5643.

Shamkhalichenar, H., Choi, J. W. (2020). Non-enzymatic hydrogen peroxide electrochemical sensors based on reduced graphene oxide. *Journal of the Electrochemical Society*, 167 (3), 037531.

Tavakoli, M., Emadi, R., Salehi, H., Labbaf, S., Varshosaz, J. (2023). Incorporation of graphene oxide as a coupling agent in a 3D printed polylactic acid/hardystonite nanocomposite scaffold for bone tissue regeneration applications. *International Journal of Biological Macromolecules*, 253, 126510.

Tingry, S., Innocent, C., Touil, S., Deratani, A., & Seta, P. (2006). Carbon paste biosensor for phenol detection of impregnated tissue: modification of selectivity by using β-cyclodextrin-containing PVA membrane. *Materials Science and Engineering: C*, 26 (2-3), 222-226.

Xu, Q., Zeng, M., Feng, Z., Yin, D., Huang, Y., Chen, Y., Yan, C., Li, R., Gu, Y. (2016). Understanding the effects of carboxylated groups of functionalized graphene oxide on the curing behavior and intermolecular interactions of benzoxazine nanocomposites. *RSC advances*, 6 (37), 31484-31496.

Xu, X., Liu, Z., Zhang, X., Duan, S., Xu, S., & Zhou, C. (2011). β-Cyclodextrin functionalized mesoporous silica for electrochemical selective sensor: Simultaneous determination of nitrophenol isomers. *Electrochimica Acta*, 58, 142-149.

Yang, C. (2004). Electrochemical determination of 4-nitrophenol using a single-wall carbon nanotube film-coated glassy carbon electrode. *Microchimica Acta*, 148, 87-92.

Yang, J. M., Hu, X. W., Liu, Y. X., & Zhang, W. (2019). Fabrication of a carbon quantum dots-immobilized zirconium-based metal-organic framework composite fluorescence sensor for highly sensitive detection of 4-nitrophenol. *Microporous and Mesoporous Materials*, 274, 149-154.

Yang, Y. L., Unnikrishnan, B., & Chen, S. M. (2011). Amperometric determination of 4-nitrophenol at multi-walled carbon nanotube-poly (diphenylamine) composite modified glassy carbon electrode. *International Journal of Electrochemical Science*, 6 (9), 3902-3912.